Supporting Information

Atomically Dispersed Fe/Co Dual Sites Electrocatalysts Derived from Covalent Triazine Frameworks for Boosting the Oxygen Reduction

Rongmin Dun [a], Xiang He [a], Jian Huang [a], Wei Wang [a], Yiwei liu [a], Linghao Li [a,b], Bowen Lu [a,b], Zile Hua [a,b,*], Jianlin Shi [a,b]

[a] State Key Laboratory of High Performance Ceramics and Superfine Microstructure, Shanghai Institute of Ceramics Chinese Academy of Sciences, 1295 Dingxi Road, Shanghai 200050, China

[b] Centre of Materials Science and Optoelectronics Engineering, University of Chinese Academy of Sciences, Beijing 100049, China

EXPERIMENTAL SECTION

All regents and chemicals are obtained commercially and used without further purification.

Synthesis of Co-N-C and Fe-N-C

1,3-dicyanobenzene (0.2 g), anhydrous $CoCl_2$ (0.1 g) and anhydrous $ZnCl_2$ (1 g) were mixed in a glove box, and then transferred into a quartz tubes, heated at the designated temperatures (400 °C) for 1 h and then (700 °C) for 20 h. The black powder was washed in 1 M HCl for 20 h, then washed with deionized water and tetrahydrofuran respectively, and finally dried in a vacuum to obtain the Co-N-C. The Fe-N-C was prepared by replacing $CoCl_2$ with anhydrous $FeBr_2$ (110 mg) under the same conditions with the Co-N-C. For comparison, the Co-N-C and Fe-N-C catalysts in this paper are all pyrolyzed at 900 °C.

Synthesis of Fe/Co-N-C

Typically, Co-N-C (100 mg) was dispersed in 10 ml isopropanol by ultrasound at room temperature for 1 h. Then the $FeCl_3 \cdot 6H_2O$ was added dropwise to the above solution under iltrasound for 30 min. Then, continue stirring the mixture at room temperature until it is dry. The powder was placed in a tube furnace and annealed at 900 ℃ for 2 h at a heating rate of 5 ℃ min^{-1} under flowing Ar gas to obtain Fe/Co-N-C.

Materials Characterizations.

The powder X-ray diffraction (XRD) patterns were collected using a Rigaku D/Max-2550 V X-ray diffractometer with a Cu Kα radiation. X-ray photoelectron

spectroscopy (XPS) spectra recorded on ESCALAB250. Raman spectra was measured on a GX-PT-1500 with a 532 nm laser excitation. The surface morphologies of the samples were obtained by transmission electron microscopy (TEM, FEI Tecnai G2 F20) and high-angle annular dark field-scanning TEM (HAADF-STEM, JEM-2100F at an acceleration voltage of 200 kV). The specific surface area was determined by the Brunauer-Emmett-Teller (BET) method using an ASAP2020 volumetric adsorption analyzer (Micromeritics, U.S.A.). The metal contents were analyzed by the inductively coupled plasma-optical emission spectrometer (ICP-OES, OPTIMA 8000).

Electrochemical Measurements.

The hydrogen peroxide yield (H_2O_2%) and the electron transfer number (*n*) were calculated by the equations:

$$H_2O_2(\%) = \frac{2I_R}{N|I_D| + I_R} \times 100$$

$$n = 4 - \left(2\frac{H_2O_2(\%)}{100}\right)$$

Here, I_D and I_R represent the disk and the ring currents; *N* is the current collection efficiency of Pt ring (0.37).

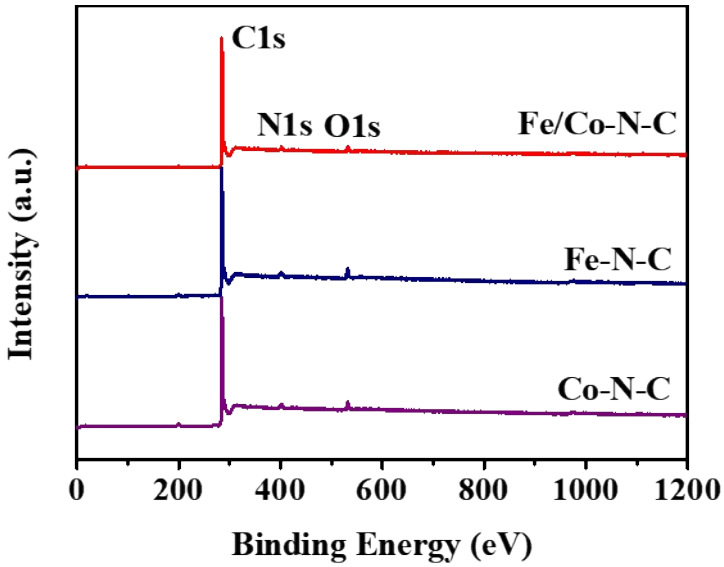

Fig. S1 Full XPS spectrum of Fe/Co-N-C, Fe-N-C and Co-N-C.

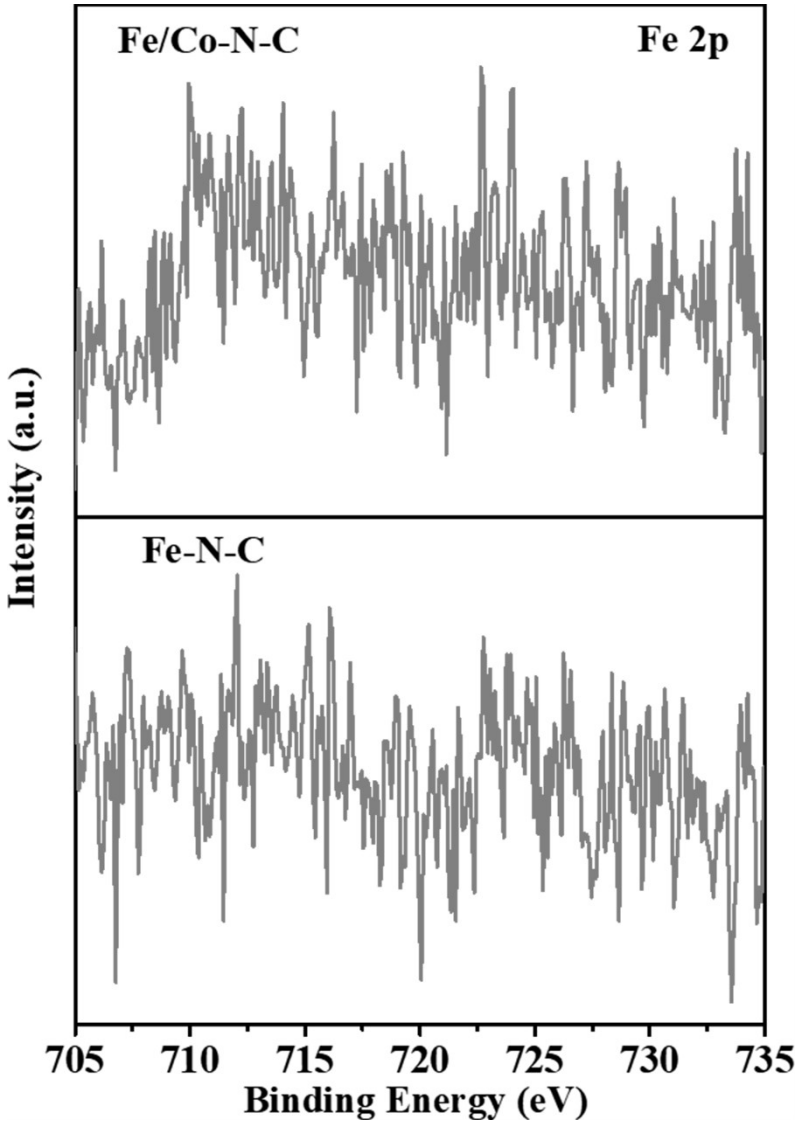

Fig. S2 Fe 2p XPS deconvolution results of Fe/Co-N-C and Fe-N-C.

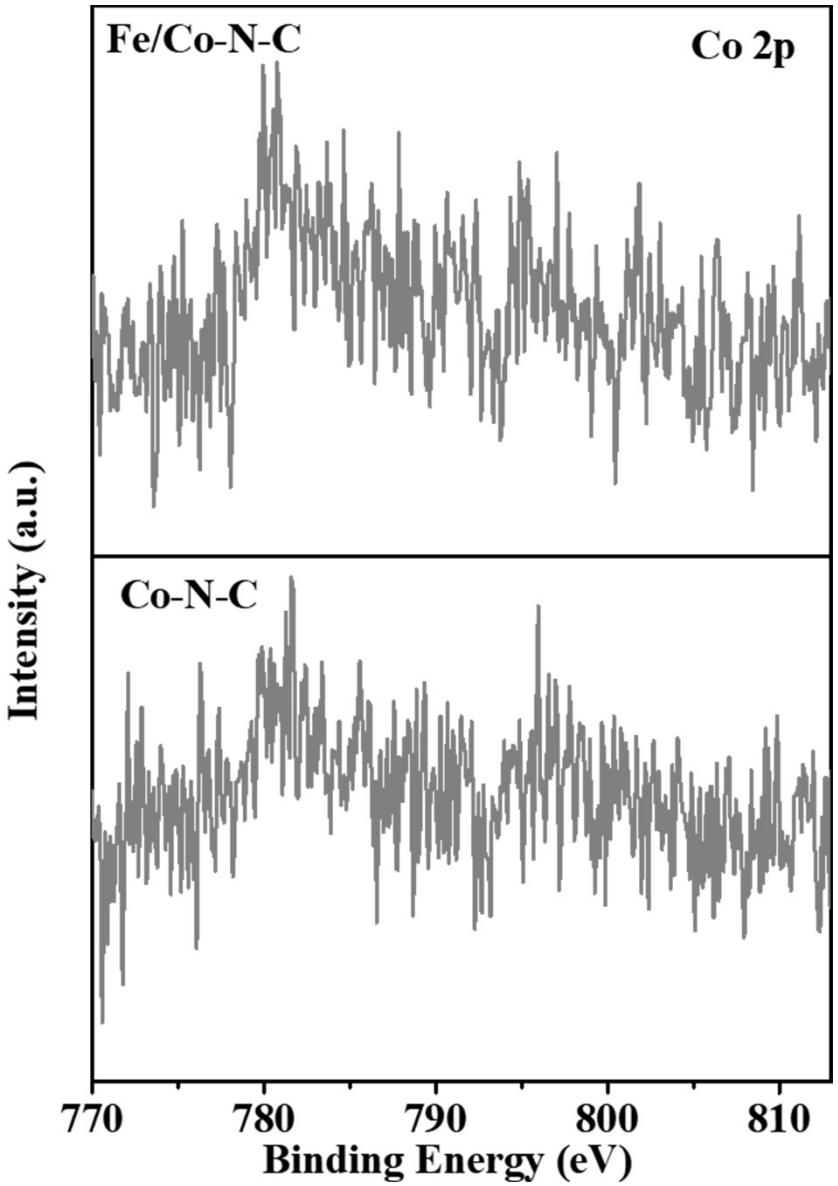

Fig. S3 Co 2p XPS deconvolution results of Fe/Co-N-C and Co-N-C.

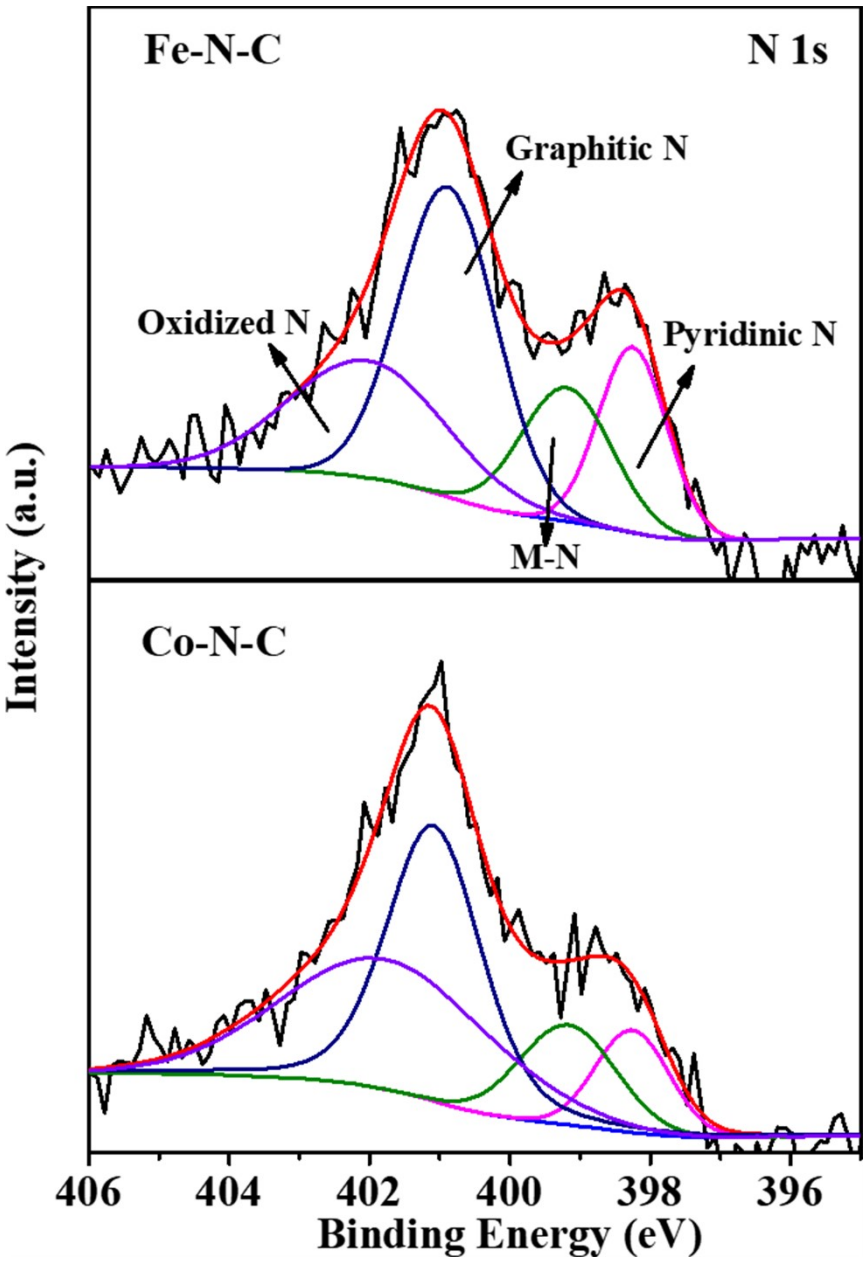

Fig. S4 N1s XPS deconvolution results of Fe-N-C and Co-N-C.

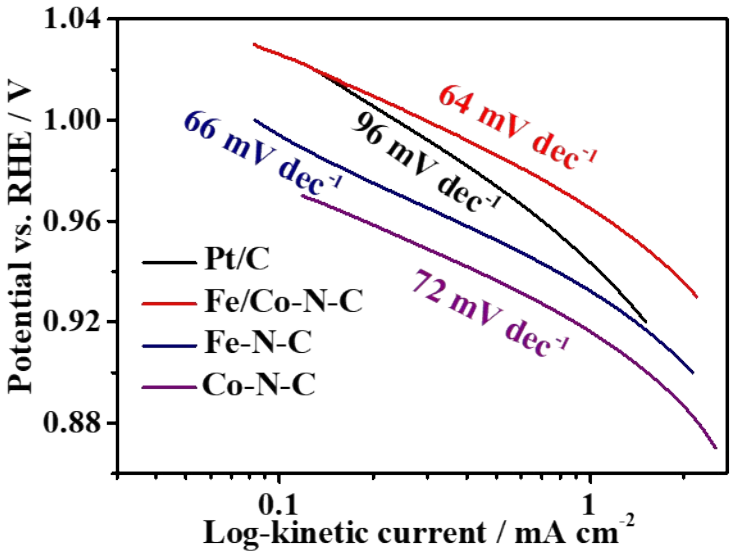

Fig. S5 Tafel plots of Pt/C, Fe/Co-N-C, Fe-N-C and Co-N-C in 0.1 M KOH.

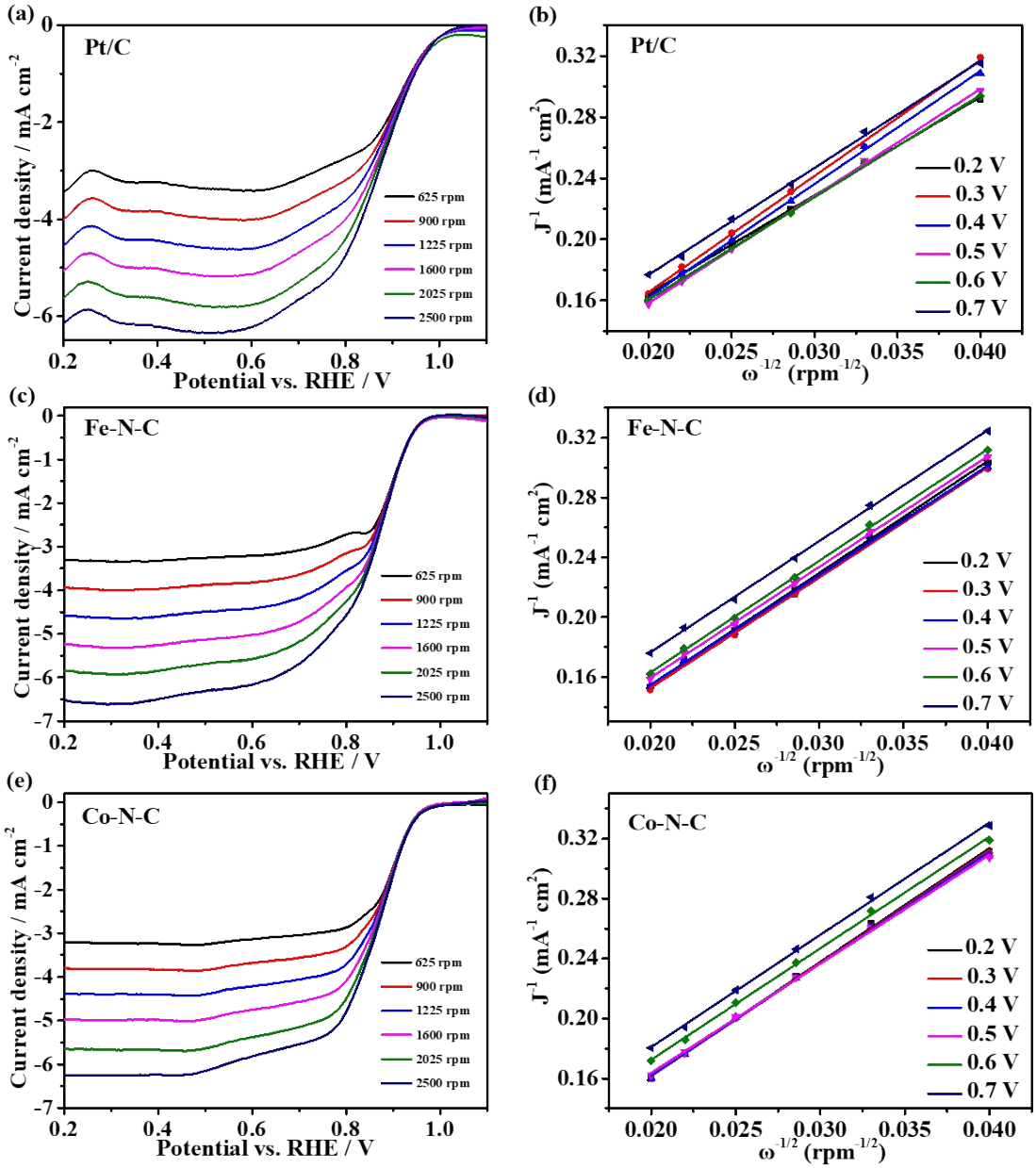

Fig. S6 (a, c, e) LSV curves of Pt/C, Fe-N-C and Co-N-C at different rotating speeds with a scan rate of 10 mV s^{-1} in O_2-saturated 0.1 M KOH solution, respectively. (b, d, f) The corresponding Koutecky-Levich plots of Pt/C, Fe-N-C and Co-N-C, respectively.

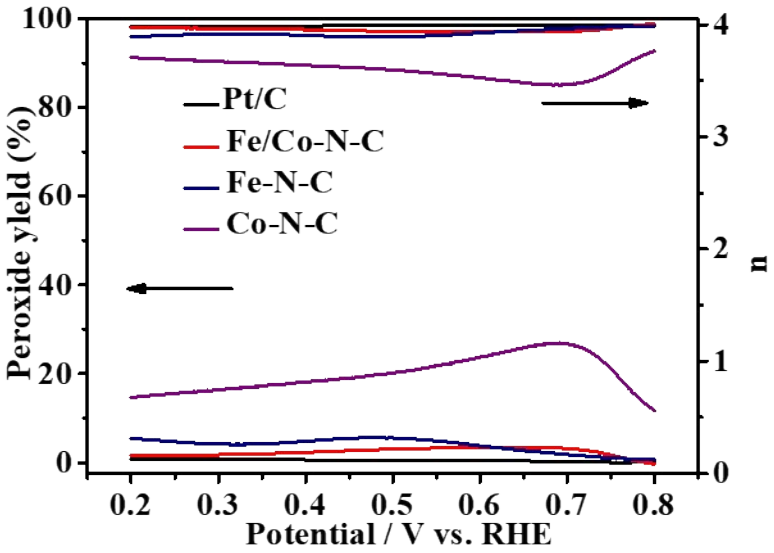

Fig. S7 H_2O_2 yield (bottom) and n (top) of different catalysts in 0.1 M KOH solution.

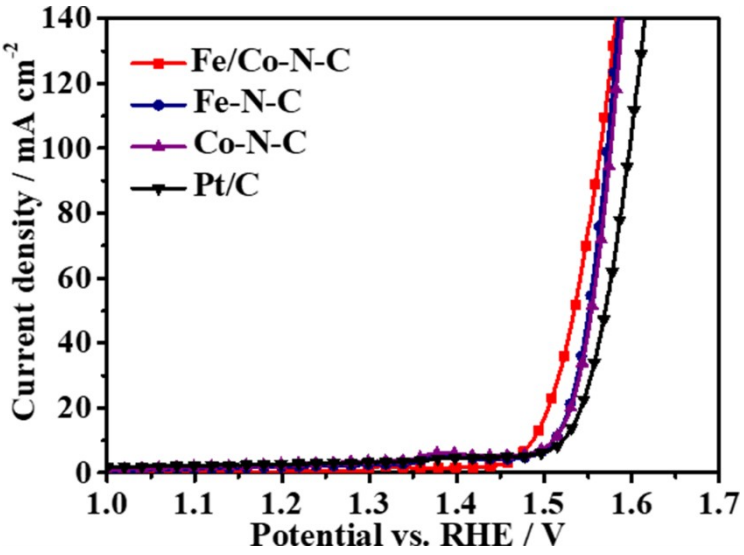

Fig. S8 Electrochemical oxygen evolution reaction activity of these catalysts in 1 M KOH solution.

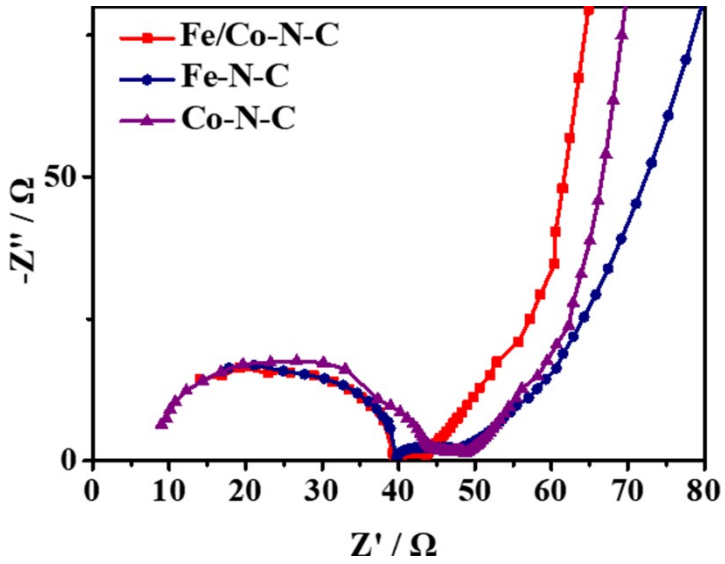

Fig. S9 The electrochemical impedance spectra of Fe/Co-N-C, Fe-N-C and Co-N-C in 0.1 M KOH electrolyte.

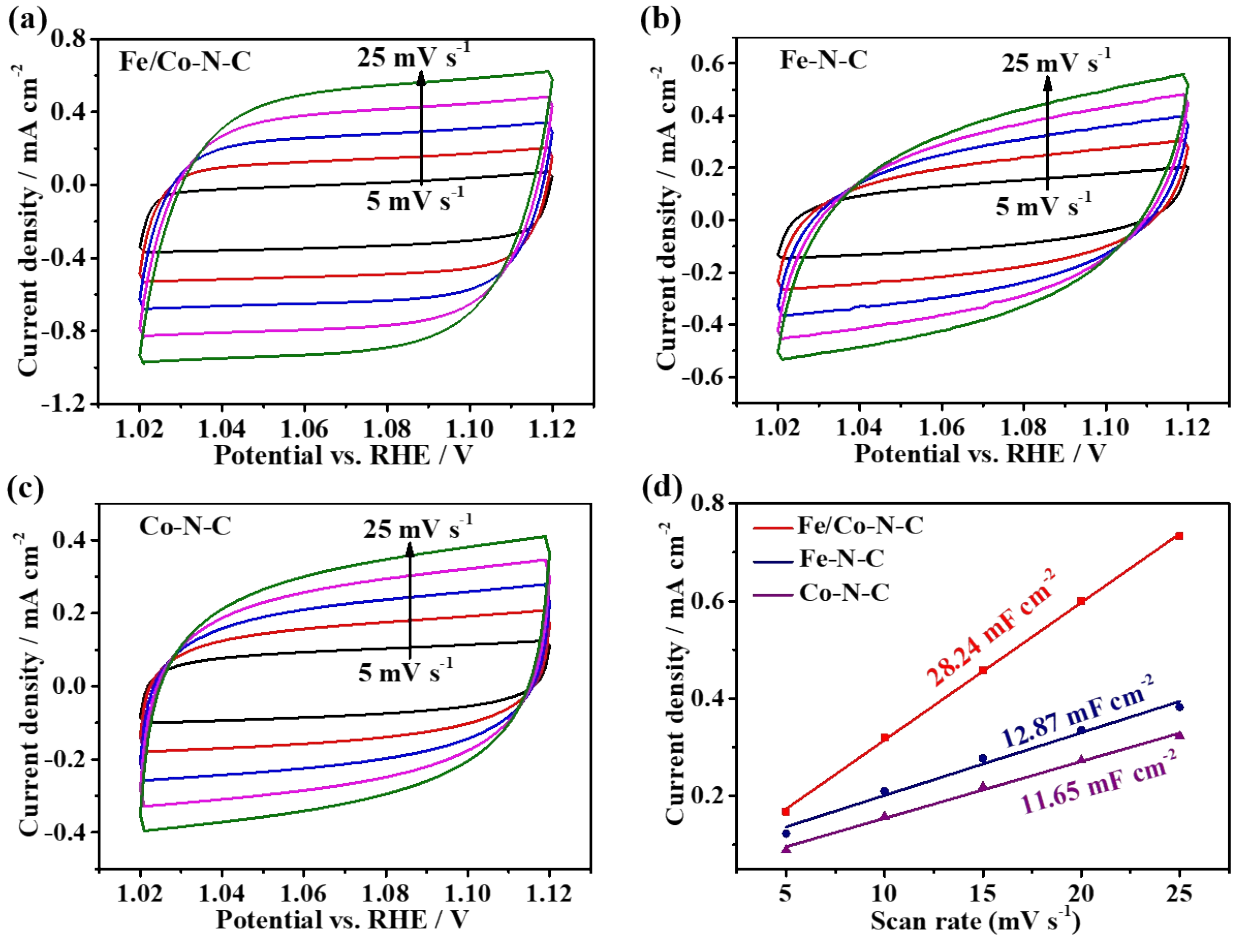

Fig. S10 Cyclic voltammetry (CV) curves of Fe/Co-N-C (a), Fe-N-C (b), Co-N-C (c) at varied with different scan rates from 5 to 25 mV·s^{-1} in a non-faradic potential range of 1.02~1.12 V *vs.* RHE in 0. 1 M KOH solution. (d) double-layer capacitance (C_{dl}) of Fe/Co-N-C, Fe-N-C and Co-N-C in 0.1 M KOH electrolyte.

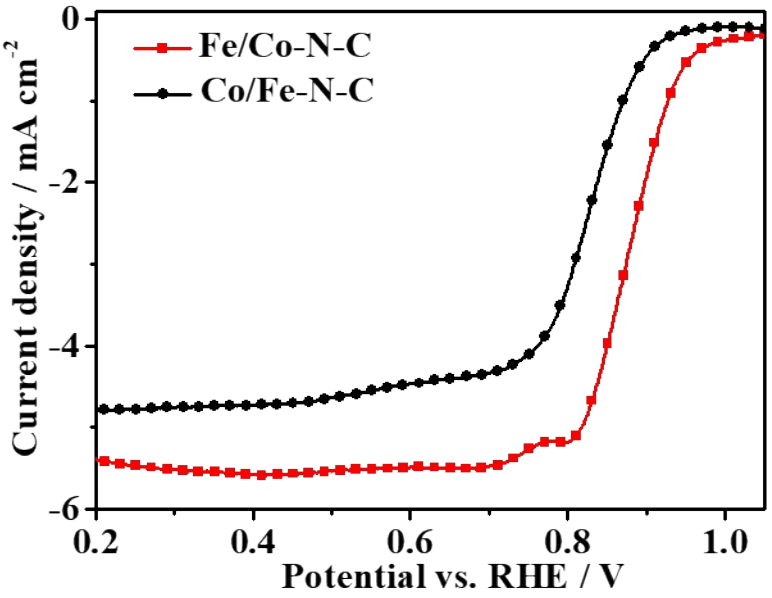

Fig. S11 LSV curves of Fe/Co-N-C and Co/Fe-N-C in O_2-saturated 0.1 M KOH solution.

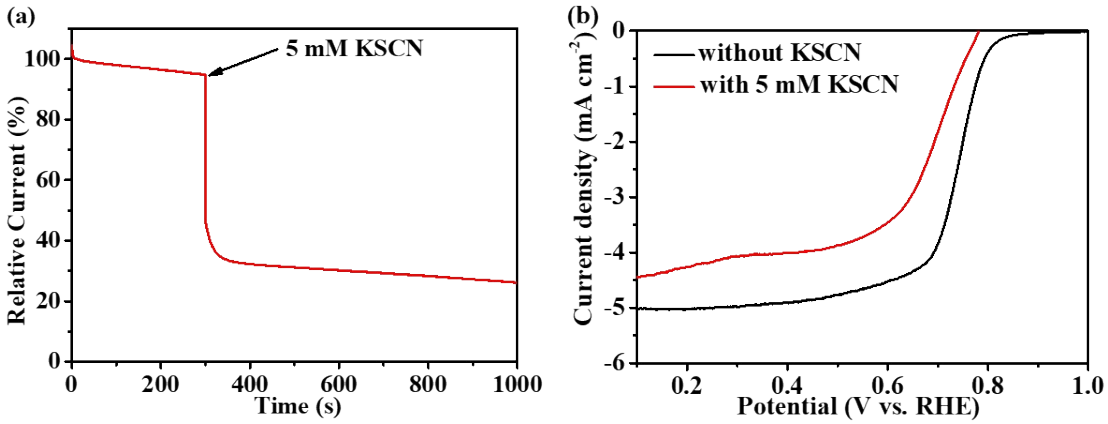

Fig. S12 (a) Current-time (I-t) curves and (b) RDE results of Fe/Co-N-C in O_2-saturated 0.1 M $HClO_4$ solution (without and with KSCN).

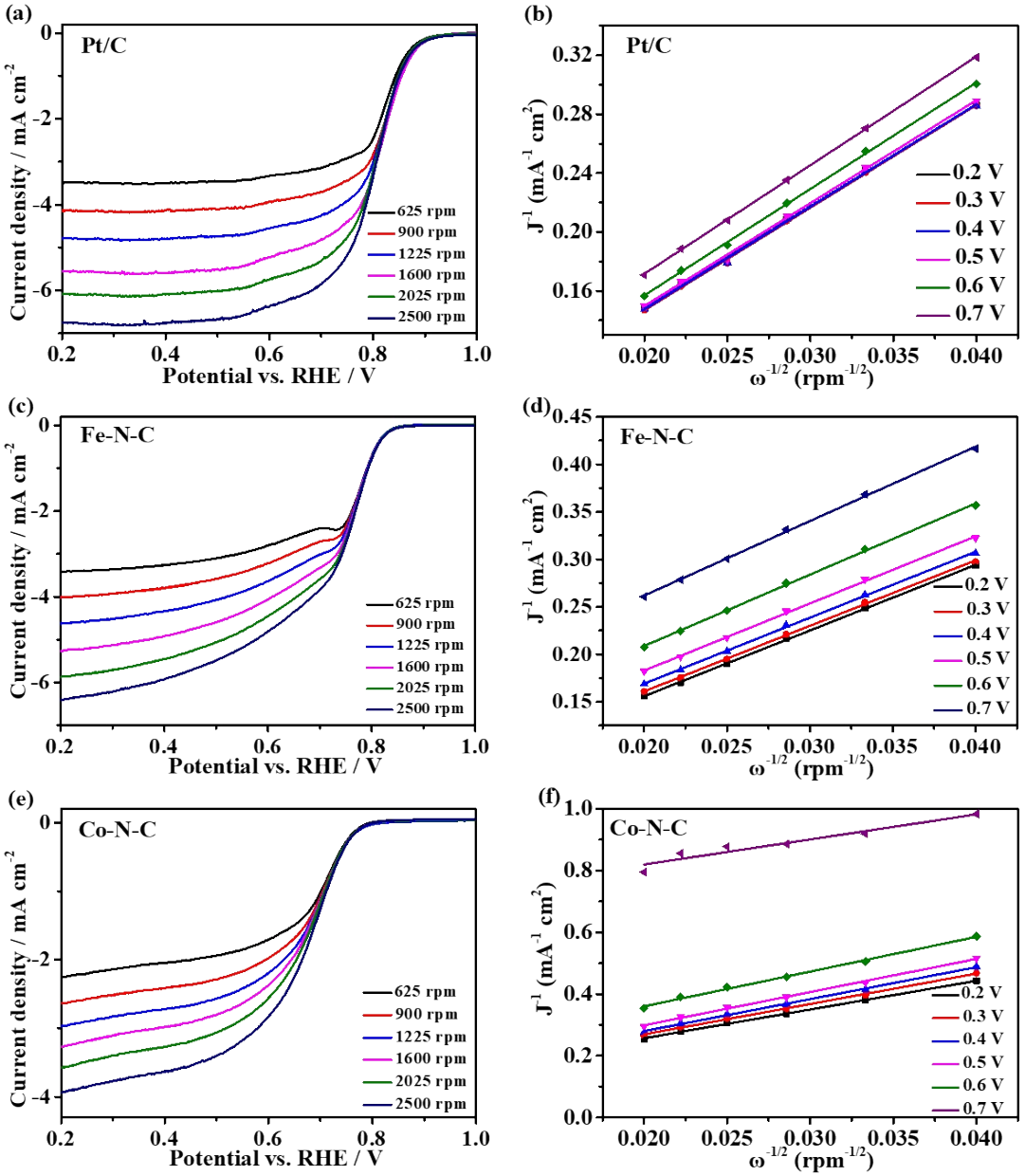

Fig. S13 (a, c, e) LSV curves of Pt/C, Fe-N-C and Co-N-C at different rotating speeds with a scan rate of 10 mV s^{-1} in O_2-saturated 0.1 M $HClO_4$ solution, respectively. (b, d, f) The corresponding Koutecky-Levich plots of Pt/C, Fe-N-C and Co-N-C, respectively.

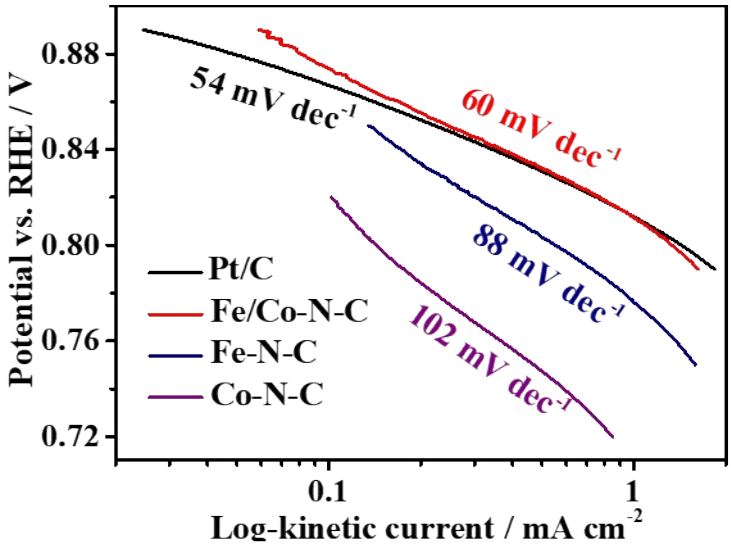

Fig. S14 Tafel plots of Pt/C, Fe/Co-N-C, Fe-N-C and Co-N-C in 0.1 M $HClO_4$.

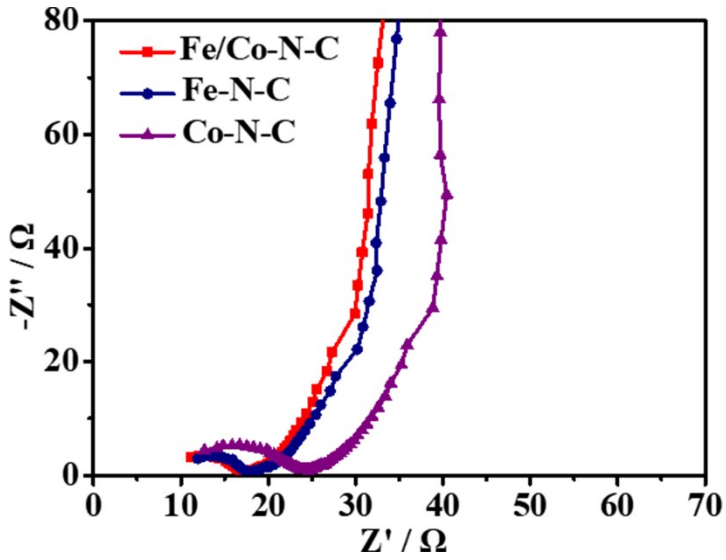

Fig. S15 The electrochemical impedance spectra of Fe/Co-N-C, Fe-N-C and Co-N-C in 0.1 M $HClO_4$ electrolyte.

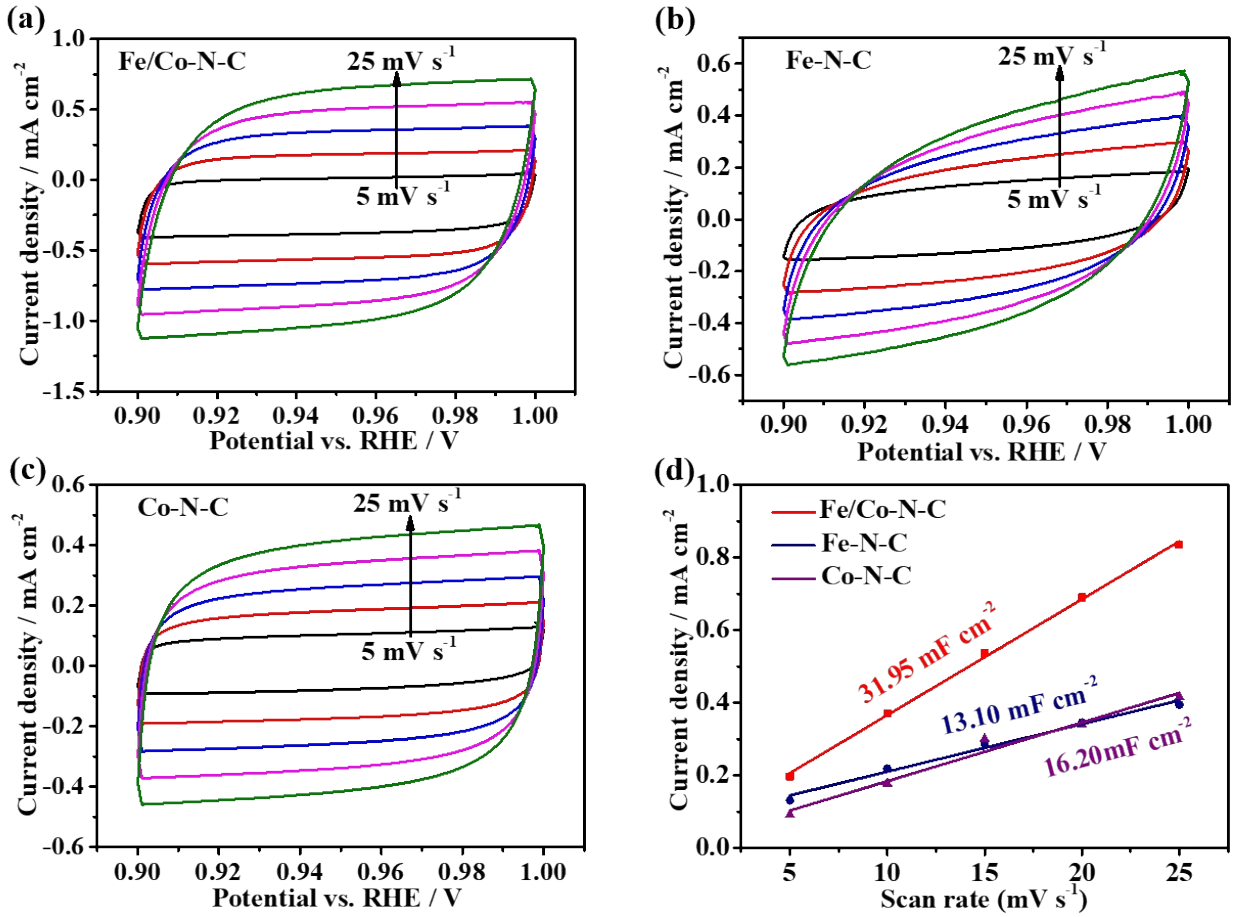

Fig. S16 Cyclic voltammetry (CV) curves of Fe/Co-N-C (a), Fe-N-C (b), Co-N-C (c) at varied with different scan rates from 5 to 25 mV·s^{-1} in a non-faradic potential range of 1.02~1.12 V *vs.* RHE in 0. 1 M $HClO_4$ solution. (d) double-layer capacitance (C_{dl}) of Fe/Co-N-C, Fe-N-C and Co-N-C in 0.1 M $HClO_4$ electrolyte.

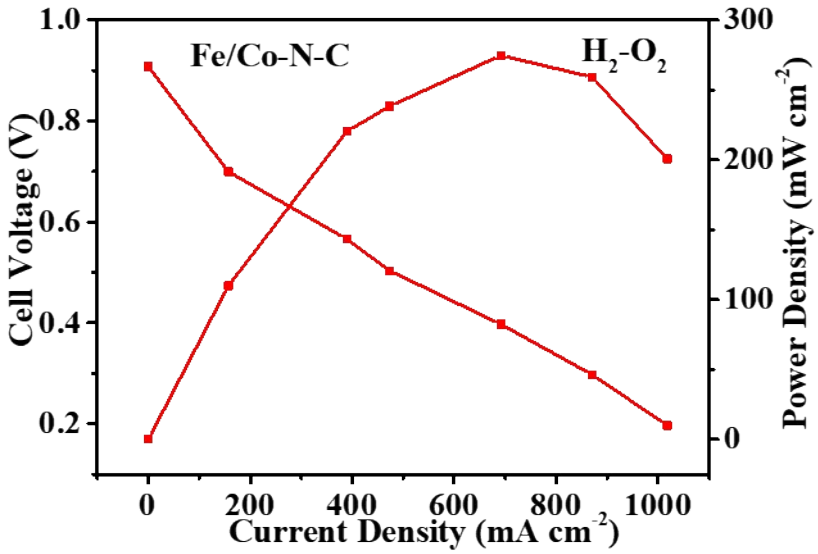

Fig. S17 Discharge polarization and power density plots of PEMFC using Fe/Co-N-C as cathode catalysts.

Table S1 Nitrogen sorption analysis results of Fe/Co-N-C, Fe-N-C and Co-N-C.

Sample	S_{BET} ($m^2\ g^{-1}$)	V_{tol} ($cm^3\ g^{-1}$)	D_{av} (nm)
Fe/Co-N-C	2447	2.4	3.5
Fe-N-C	2405	2.0	3.2
Co-N-C	2324	2.5	3.8

Table S2 The XPS element content of Fe/Co-N-C, Fe-N-C and Co-N-C.

Sample	C(at.%)	N(at.%)	O(at.%)	Fe(at.%)	Co(at.%)
Fe/Co-N-C	91.08	2.19	6.18	0.21	0.34
Fe -N-C	91.92	2.95	4.96	0.17	-
Co-N-C	90.91	2.78	6.13	-	0.18

Table S3 The metal content of Fe/Co-N-C, Fe-N-C and Co-N-C measured by ICP-OES.

Sample	Fe(wt.%)	Co(wt.%)
Fe/Co-N-C	1.80	0.92
Fe -N-C	0.27	-
Co-N-C	-	0.63

Table S4. The electrocatalytic activities of Fe/Co-N-C and some recently reported NMP catalysts for ORR in 0.1 M KOH or NaOH solution.

Catalyst	Electrode rotation speed (rpm)	Half-wave potential (mV)	Catalyst loading (mg cm^{-2})	Reference
Fe/Co-N-C	1600	922	0.4	This work
Co-N_3-C	1600	891	0.26	S1[1]
FeN_4-PN	1600	910	0.2	S2[2]
Fe-Nx/C	1600	910	0.71	S3[3]
Co-TMPyP/CCG	1600	824	0.25	S4[4]
Co@N, S–C	1600	894	0.6	S5[5]
Cu/Zn-NC	1600	830	0.4	S6[6]
ZFN-900	1600	850	-	S7[7]
Zn_6Co	1600	890	0.5	S8[8]

Table S5. The electrocatalytic activities of Fe/Co-N-C and some recently reported NMP catalysts for ORR in acidic media.

Catalyst	Electrode rotation speed (rpm)	Half-wave potential (mV)	Catalyst loading (mg cm^{-2})	Reference
Fe/Co-N-C	1600	769	0.4	This work
Fe-N-C-1	1600	743	0.5	S9[9]
Fe-N-GC-900	1600	740	0.6	S10[10]
FeNC-900	1600	720	0.2	S11[11]
Fe_3C/C-700	900	730	0.6	S12[12]
Co-N-GA	1600	730	0.6	S13[13]

References

1 H. Xu, H. Jia, H. Li, J. Liu, X. Gao, J. Zhang, M. Liu, D. Sun, S. Chou, F. Fang and R. Wu, *Appl. Catal., B*, 2021, **297**, 120390.

2 Y. Lin, K. Liu, K. Chen, Y. Xu, H. Li, J. Hu, Y.-R. Lu, T.-S. Chan, X. Qiu, J. Fu and M. Liu, *ACS Catal*., 2021, **11**, 6304-6315.

3 G. Li, J. Yang, Y. Chen, M. Liu, X. Guo, G. Chen, B. Chang, T. Wu and X. Wang, *ACS Appl. Mater. Interfaces*, 2021, **13**, 54032-54042.

4 K. Cui, Q. Wang, Z. Bian, G. Wang and Y. Xu, *Adv. Energy Mater*., 2021, **11**, 2102062.

5 D. Lyu, S. Yao, A. Ali, Z.Q. Tian, P. Tsiakaras and P.K. Shen, *Adv. Energy Mater*., 2021, **11**, 2101249.

6 M. Tong, F. Sun, Y. Xie, Y. Wang, Y. Yang, C. Tian, L. Wang and H. Fu, *Angew. Chem. Int. Ed*., 2021, **60**, 14005-14012.

7 A. Radwan, H. Jin, B. Liu, Z. Chen, Q. Wu, X. Zhao, D. He and S. Mu, *Carbon*, 2021, **171**, 368-375.

8 Y. Xiong, Y. Yang, F.J. DiSalvo and H.D. Abruna, *J. Am. Chem. Soc*., 2019, **141**, 10744-10750.

9 J. Li, S. Chen, N. Yang, M. Deng, S. Ibraheem, J. Deng, J. Li, L. Li and Z. Wei, *Angew. Chem. Int. Ed*., 2019, **58**, 7035-7039.

10 A. Kong, X. Zhu, Z. Han, Y. Yu, Y. Zhang, B. Dong and Y. Shan, *ACS Catal*., 2014, **4**, 1793-1800.

11 Q. Zuo, P. Zhao, W. Luo and G. Cheng, *Nanoscale*, 2016, **8**, 14271-14277.

12 Y. Hu, J.O. Jensen, W. Zhang, L.N. Cleemann, W. Xing, N.J. Bjerrum and Q. Li, *Angew. Chem. Int. Ed*., 2014, **53**, 3675-3679.

13 X. Fu, J.Y. Choi, P. Zamani, G. Jiang, M.A. Hoque, F.M. Hassan and Z. Chen, *ACS Appl. Mater. Interfaces*, 2016, **8**, 6488-6495.